An investigation of the field-induced ferrielectric subphases in antiferroelectric liquid crystals

1995 J. Phys.: Condens. Matter 7 L351

(http://iopscience.iop.org/0953-8984/7/27/001)

J. Phys.: Condens. Matter 7 (1995) L351–L360. Printed in the UK

LETTER TO THE EDITOR

An investigation of the field-induced ferrielectric subphases in antiferroelectric liquid crystals

Yu P Panarin†, H Xu†, S T MacLughadha†, J K Vij†§, A J Seed‡, M Hird‡ and J W Goodby‡

† Department of Microelectronics and Electrical Engineering, University of Dublin, Trinity College, Dublin 2, Ireland

‡ School of Chemistry, University of Hull, Cottingham Road, Hull, HU6 7RX, UK

Received 24 May 1995

Abstract. We report results of detailed investigations of the dielectric response of two antiferroelectric liquid crystal materials over a wide range of frequencies as a function of bias voltage and of temperature. On the basis of extensive measurements of the tilt angle, the spontaneous polarization, and the optical transmittance as a function of voltage, we conclude that there appears to exist a previously undetected, new field-induced phase (referred to as the X phase) with uniform monodomain structure. This new phase seems to be stable over a wide range of applied voltages and possesses effective values of spontaneous polarization and tilt angle within 70–80% of their maximum values. Although the results appear to rule out the presence of the SmC_{α}^{*} phase, nevertheless, the new phase has some characteristics similar to those of the SmC_{α}^{*} phase. The differences between the characteristics of the two phases are detailed.

Although Beresnev *et al* [1] predicted the existence of an antiferroelectric structure in an FLC mixture in 1988 to explain its unusual dependence of the pyroelectric properties with temperature, a detailed study of antiferroelectric liquid crystals (AFLCs) did not commence until Chandani *et al* [2] in 1989 discovered their ability for tristable electrooptical switching. Later from conoscopic investigations various other ferrielectric subphases were also discovered in the temperature range between the AFLC and the SmA phases [3]. The appearance of these subphases can be understood to be as a result of the competition between the antiferroelectric and ferroelectric interactions in adjacent smectic layers, which stabilize the SmC_A and SmC^* phases. This competition produces various ferrielectric subphases responsible for the Devil's staircase. These phases can be characterized by the parameter q_T denoting the fraction of ferroelectric ordering which appears in the antiferroelectric structure. Several different theoretical approaches [4–8] have been developed to explain the Devil's staircase. These theories explain the sequence of transitions between antiferroelectric, ferrielectric and ferroelectric phases with changing temperature and/or applied voltage. It follows from these theories that the maximum value of the spontaneous polarization in the ferrielectric phases is equal to one-third of the value of the spontaneous polarization in the ferroelectric phase. The SmC_{α}^{*} phase is different and its existence and properties cannot be explained using the aforesaid models. The complete investigation of the electric field versus temperature (E–T) phase diagrams provided by Isozaki *et al* [8] on different binary

§ Author to whom correspondence should be addressed.

0953-8984/95/270351+10$19.50

mixtures shows that the SmC^*_α phase appears in the temperature range below the SmA and borders with the SmC^*, AF or SmC^*_γ phases. The electric-field-induced polarization and tilt angle for the SmC^*_α phase can significantly exceed the maximum ferrielectric value of order one-third. As follows from E–T phase diagrams [8] the application of electric field in the SmC^* phase causes only helix unwinding but not any other ferri–antiferroelectric phase transition.

Detailed dielectric and electro-optic data have not been provided in previous investigations [8–10]. Observation of some AFLC sample using a polarizing microscope provides evidence for the existence of an unknown quasistable phase [11] which exists under applied bias voltage conditions over a wide temperature range corresponding to the SmC^*_A. We found that this subphase exists also in the SmC^*_γ and SmC^* phases. This phase exhibits unusual dielectric and electro-optical properties which are significantly different to the properties of AF and FI phases and are to some extent similar to the properties of SmC^*_α. Later we will show the results of electro-optical and dielectric investigations of two AFLC samples that possess this phase.

We present investigations of two AFLC samples under high bias voltages for the cells of thicknesses 4–20 μm. The samples used in experiments were AS-425 and As-573 (Hull, UK) possessing the following phase transition sequences

AS-425: Cr–80.3–SmC^*–91.3–SmC_α–91.3–$TGBA^*$–95.6–IS

(on cooling: SmC^*–48.2–SmC_γ–39.5–SmC_A)

AS-573: SmC_A–78.3–SmC_γ–82–SmC^*90.7–SmA–105.7–Is.

(transition temperatures are in °C)

Phase transition temperatures were measured using differential scanning calorimetry (DSC). Sample cells consisted of ITO-coated glass plates. The conducting inner surfaces were spin coated with a polyvinyl alignment layer and rubbed parallel. The cells were filled in the isotropic phase. Textures of the experimental cells were observed using a polarizing microscope. Dielectric measurements, in the frequency range 1 Hz–1 MHz were made using a Schlumberger 1255 frequency response analyser and a Chelsea dielectric interface. This system enabled us to apply direct bias voltages up to 40 V and an alternating measuring voltage up to 3 V rms simultaneously to samples during measurements. The dielectric measurements were carried out on the homogeneously aligned (planar) samples; therefore providing $\varepsilon_\perp$ and the optical textures could be simultaneously observed through a polarizing microscope. Birefringence measurements were performed using a Leitz tilting compensator fitted to a Leitz Wetzlar polarizing microscope. This device enables us to measure the phase difference, experienced by light as it passes through a birefringent material. It was possible to measure the dependence of the effective birefringence Δn on both temperature and applied bias voltage. The spontaneous polarization was measured using the integral reversed current method [12].

We studied the dielectric response of both AFLC samples in cells of the following thicknesses: 6, 10, 20 μm. The experimental dielectric spectra are found to be practically independent of the cell thickness, therefore we shall present the typical experimental results for a cell with 10 μm spacing.

The field-induced subphase exists in both samples, however as the sample AS-573 possesses no $TGBA^*$ phase high-quality alignment can be more easily achieved. For this reason this material is investigated in greater detail. The optical contrast ratio in this case in a 10 μm cell achieved values of 50:1 to 100:1 and this enables us to make precise electro-optical and birefringence measurements.

Because the samples investigated reveal properties similar to the SmC_α^* phase we concentrated on the identification of the phase that was found from DSC measurements to be SmC* in the temperature range 82–90 °C. Neither optical texture nor conoscopic observations are usually effective for the identification of the SmC_α^* phase [10]. However dielectric spectroscopy without bias field can better determine the phase transition temperatures [13] and complement the results of DSC. Figure 1 presents the dependence of the dielectric loss spectra on temperature. According to this plot only the SmC* phase is seen to exist in the temperature range 82–90 °C and no other phase transitions are observed in this temperature interval.

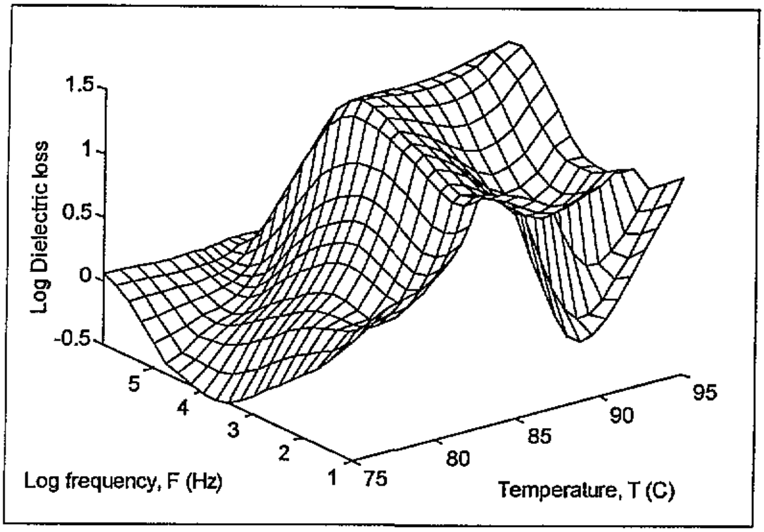

Figure 1. Dielectric loss spectra versus temperature for AS-573, $d = 10$ μm.

The temperature dependence of the dielectric parameters of AS-573 under the absence of a direct bias voltage is shown in figure 2. It should be noted that two relaxation processes in the dielectric spectra in this temperature range are observed. The high-frequency process is the Goldstone relaxation of the helical structure. This assignment follows from the analysis of the temperature dependence of the dielectric relaxation strength (figure 2). The temperature dependence follows the usual conversion from the soft mode in SmA phase to the Goldstone mode in SmC* phase. The soft mode is dominated by the Goldstone mode in the SmC* phase. In addition to the Goldstone process being discussed, another relaxation process appears 2–3 °C below the SmA–SmC* phase transition and is also seen to exist in both SmC_γ^* and SmC_A phases. The mechanism of this relaxation process is not yet completely clear but seems to be the ferrielectric Goldstone mode for the reasons given below.

Recently Cepic *et al* [15] developed a phenomenological theory describing the dynamical behaviour and the dielectric spectra of different $SmC_A(q_T)$ subphases. This model predicts that below the phase transition temperature $SmC^* \rightarrow SmC_\gamma^*$, the relaxation time of the Goldstone mode decreases by one to two orders of magnitude and the dielectric

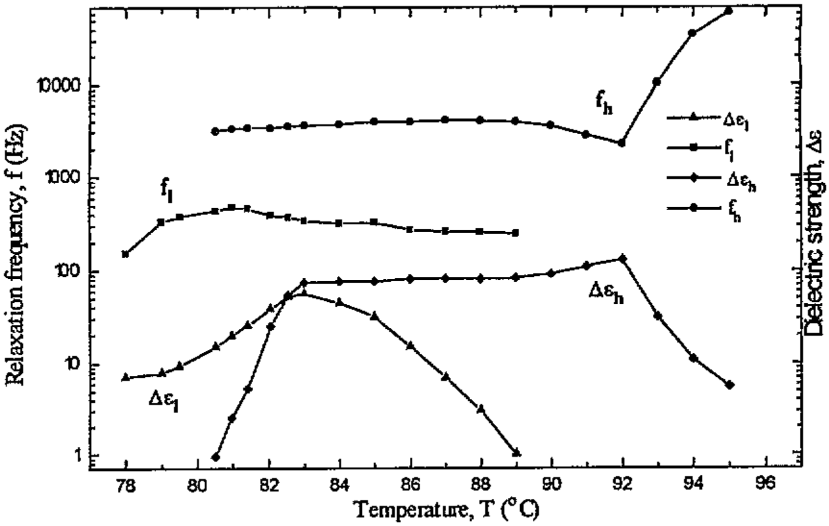

Figure 2. The dependence of the dielectric parameters ($\Delta\varepsilon$, f) on temperature for AS-573, $d = 10$ μm, on cooling.

strength increases by several orders of magnitude. In both SmC* and SmC^*_γ phases only one relevant relaxation process is seen. This behaviour has been observed experimentally in MHPOBC [13]. However the dielectric spectrum of the AS-573 sample in the SmC* phase possesses two relaxation processes: one is the ferroelectric Goldstone mode and another can be assigned to the ferrielectric mode because it also exists in the SmC^*_γ phase and its relaxation frequency is one order less than the relaxation frequency of the SmC* Goldstone mode [13, 14]. The existence of these two relaxation modes is not in agreement with theoretical models that have so far been developed. The existence of these processes can possibly be explained by the importance of the antiferroelectric interactions in the SmC* phase.

The application of the bias voltage considerably changes the dielectric spectra (figure 3). An increase in the bias voltage suppresses the low-frequency relaxation mode and causes the high-frequency process initially to increase with voltage, followed by a decrease in the amplitude with an increase in voltage.

In order to explain the unusual dielectric properties observed for the sample we made electro-optical and effective polarization measurements and polarizing microscopy observations of the texture. The dependence of the normalized spontaneous polarization $P_s(V)/P_s$ on applied voltage for different temperatures (phases) shown in figure 4 exhibits several interesting features.

As seen from figure 4, the shape of the curves depends not only on the phase but also on the temperature within the same phases. The three curves 90, 88, 83 °C correspond to the SmC* phase but these exhibit different shapes. At 90 °C the curve shows a typical dependence of polarization on voltage for a helical SmC* cell. At low voltages, the effective polarization is found to be linearly related to the voltage and this corresponds to a distortion of the helix. At higher voltages, the normalized polarization reaches the saturation value of the unwound SmC* structure. From figure 2, we observe, as expected, at this temperature the cell exhibits only one dielectric relaxation process. At lower temperatures (83–88 °C), the voltage dependence of the effective polarization exhibits an intermediate metastable phase. The average value of effective polarization for the intermediate metastable phase

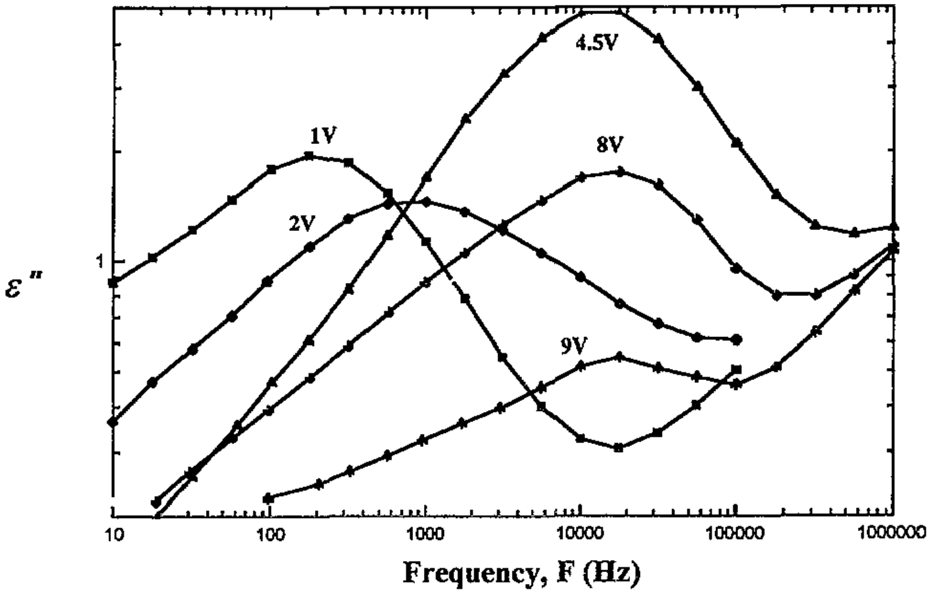

Figure 3. Dielectric loss spectra versus bias voltage for AS-573, 10 μm cell.

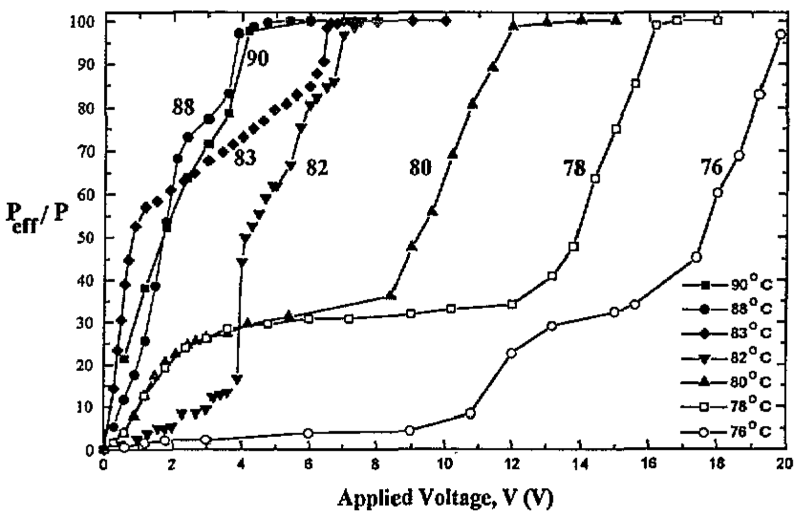

Figure 4. The temperature dependence of the normalized spontaneous polarization as function of applied voltage for different phases: SmC*—90, 88, 83 °C; SmC^*_γ—82, 80, 78 °C; SmC^*_A—76 °C.

is equal to 75% of the maximum polarization for the unwound helix. The stability of this phase increases with a decrease in temperature down to SmC*–SmC^*_γ. This phase could not be assigned to the field-induced FiLC phase because the average of polarization exceeds the known maximum value of Ps/3 for ferrielectric phases as shown in figure 4 for the curves corresponding to SmC^*_γ and SmC_A phases. Another specific property of this field-induced metastable phase is 'flexibility' i.e. a quite strong linear dependence of the induced polarization on voltage. The property of a linear dependence of P on E with a large value of dP/dE gives a high value of dielectric strength with bias voltages (figure 3). This metastable phase exists also in the electro-optical response, as shown in figure 5 where the shape of the hysteresis at 86 °C shows a step in transmittance with voltage not normally observed for the SmC* phase.

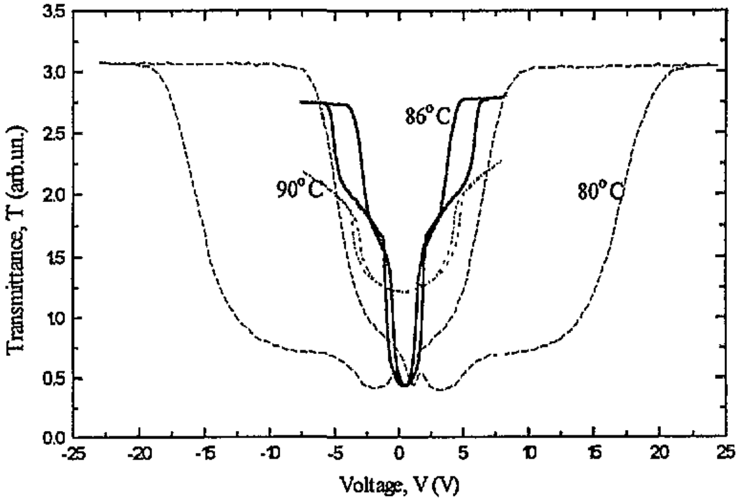

Figure 5. The optical hysteresis of AS-573 for different temperatures, $d = 10\ \mu$m, $f = 0.02$ Hz. The smectic layer normal was along the polarizer axis. Dashed curve, 80 °C, chain curve, 90 °C; continuous curve, 86 °C (note the step in the hysteresis for $V = \pm 2.5$ V).

Figure 6 presents the temperature–voltage (T–V) phase diagram deduced from the texture changes observed with a 10 μm AS-573 cell and those obtained from P_s measurements presented in figure 4. From figure 6, we found that the field-induced metastable phase exists in all of the tilted smectic phases. It is found to be most stable in the SmC* phase just above the SmC*–SmC$^*_\gamma$ temperature transition. The structure of this metastable phase is under investigation. We remark that such a metastable phase is not the property of a specific substance but has also been observed for another compound, AS-425.

Figure 7 shows the plot of the dielectric relaxation strength as a function of the bias voltage for AS-425. We find that the number of peaks and their shape depend on the temperature. The peak exhibited at low bias voltages corresponds to the helix unwinding process with applied voltage and appears for all temperatures in the SmC* and SmC$^*_\gamma$ phases. After the helix is unwound the Goldstone mode must be suppressed by the bias voltage as in the case of $T = 70$ °C. It should be noted that the dielectric spectra in the absence of direct bias voltage in the temperature range 50–80 °C possess similar behaviour to the DSC data and this confirms the existence of only one SmC* phase at these temperatures. Thus at the lower temperatures of 60 °C and 50 °C the sample is still in the SmC* phase; however, the sample does exhibit two peaks. We made electro-optical and spontaneous polarization measurements to supplement dielectric data for this phenomenon. Figure 8 presents the dependence of the transmittance, the optical switching angle (θ) and the effective polarization on applied voltage for the 10 μm cell at 50 °C.

Textures of the cells were observed using a polarizing microscope during the dielectric measurements. At low values of the applied/bias voltage the cell possesses helical structure,

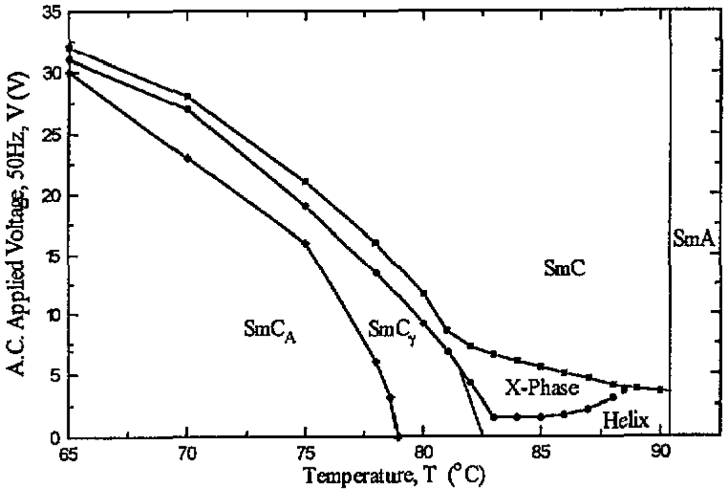

Figure 6. The temperature–voltage phase diagram of AS-573 in the 10 μm cell.

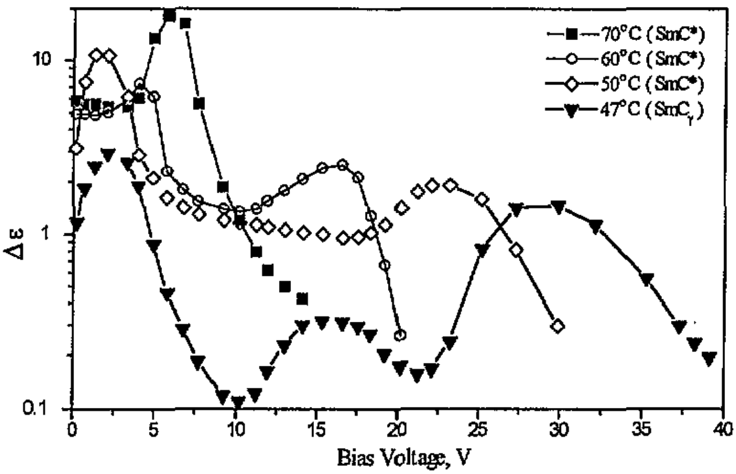

Figure 7. The dependence of the total dielectric strength, ΔE, on bias voltage.

and for large values of applied voltage (>20 V) the unwound SmC uniform state is seen. Over a wide range of intermediate values (7–16 V), we observe a uniform monodomain structure (which we term as the X phase). This phase possesses interesting properties. The effective values of the spontaneous polarization and tilt angle are within 70–80% of the values of the unwound SmC state and this significantly exceeds the maximum value (one-third) for the ferrielectric phases. Such behaviour is similar to SmC$^*_\alpha$ [15]. The birefringence of this structure is found to be slightly dependent on voltage. Between these structures (helical, X structure and SmC*) the cell possesses a mixture of different textures as indicated in figure 9. At a temperature of 47 °C and under various applied voltages, the cell exhibits four textures as observed under a polarizing microscope: helical ferrielectric (SmC$^*_\gamma$, $q_T = \frac{1}{3}$), unwound ferrielectric, X structure and SmC. The peaks in the curve for the dependence of the dielectric strength on bias voltage (figure 1) correspond to the

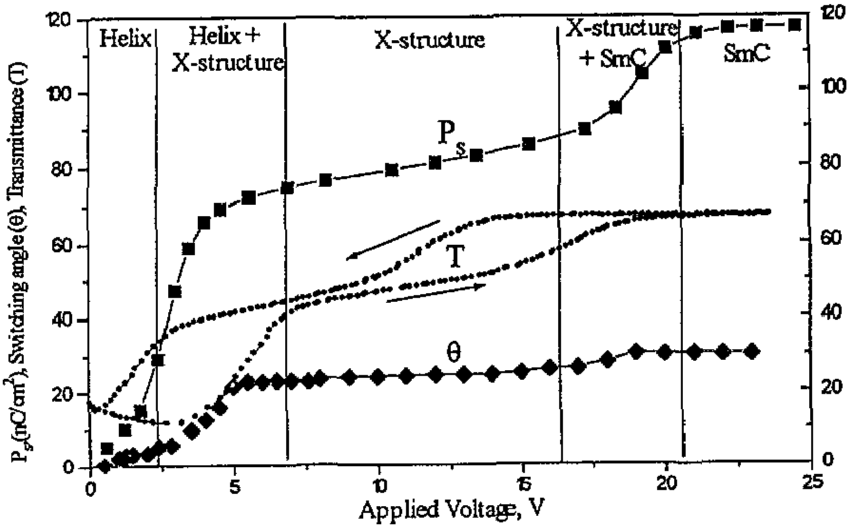

Figure 8. The dependence of the transmittance, the optical switching angle (θ) and the effective polarization (P) on applied voltage for a 10 μm cell at 50 °C.

domain wall motion between different textures and thus the number of the peaks is equal to the number of possible textures minus one. Figure 9 presents the T–V (temperature–voltage) phase diagram for the sample AS-425 in a 10 μm thick cell produced by polarizing microscopy texture observations.

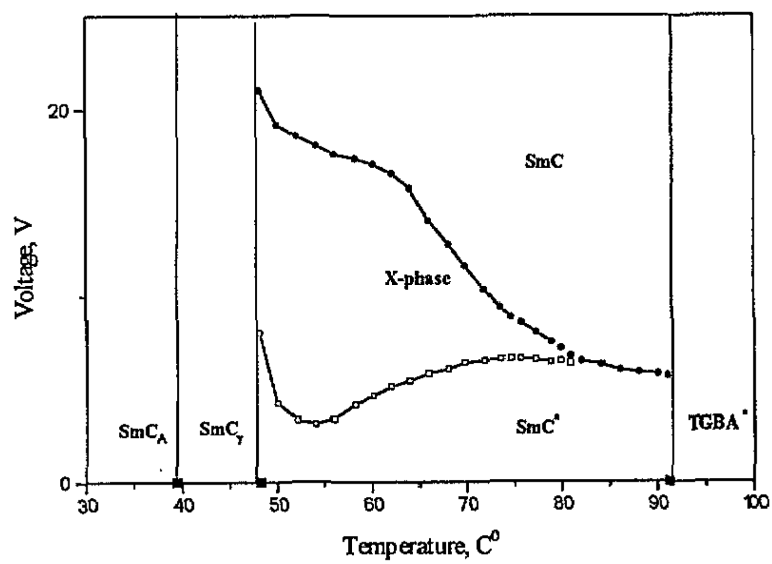

Figure 9. The temperature–voltage phase diagram of AS-425 (d = 10 μm).

The metastable phase is found to exist in both AFLC materials studied in this work. As has already been shown, the X phase possesses most interesting properties, which are different from those of ferroelectric and ferrielectric phases. The existence of this structure does not follow the current theories which describe the 'Devil's staircase' observed in the ferrielectric phase. The main contradictions are as follows.

(i) The field-induced polarization and tilt angle for this metastable phase are much higher than the maximum value of one-third for ferrielectric subphases in the Devil's staircase and achieve the value of 85% of SmC* phase.

(ii) In contrast with field-induced ferrielectric phases ($\frac{1}{2} < q_T(E) < 1$) in which all parameters are practically independent of applied voltage the metastable phase called the X phase exhibits 'flexibility', i.e. quite strong linear dependence on voltage.

(iii) As follows from T–V diagrams for various AFLC mixtures [8] the application of the external electric field cannot cause any ferri/antiferroelectric phases.

Under the above-mentioned consideration this metastable phase could not be assigned to the known (q_T or q_E) ferrielectric phases.

The properties of the metastable phase seems to be similar to the properties of SmC^*_α [15]. The values of induced tilt angle and spontaneous polarization in SmC^*_α can also considerably exceed the value of one-third. Moreover there are some features which distinguish this phase from SmC^*_α. Careful comparison of the properties of SmC^*_α and the X phase shows several differences.

(i) In SmC^*_α the level of the induced tilt angle is strongly dependent on temperature [16]. In the X phase the middle value of induced polarization/tilt angle is always approximately 75% of the maximum value.

(ii) In SmC^*_α the dependence of induced tilt angle on voltage exhibits steplike behaviour [15], in the X phase this dependence is linear.

(iii) According to the conventional point of view [8, 10], no field-induced transitions from SmC* to SmC^*_α are possible.

Thus we can conclude that the X phase is different from the SmC^*_α phase.

Concerning the structure of the X phase it could be useful to consider the collective polarization fluctuations as proposed by Prost and Bruinsma [7]. These fluctuating forces cause the antiferroelectric order in the adjacent smectic layers and are responsible for antiferroelectricity in the SmC^*_α phase. Because of these fluctuations, the antiferroelectric order in this phase is not completely coherent as in $\mathrm{SmC_A}$ and this could be easily affected by the electric field. Sufficiently high values of the induced tilt angle/polarization in the X phase (55–85%) and especially its 'flexibility' suggest that the antiferroelectricity has no strict order and its reduction in the order with increasing the electric field may account for the appearance of the X phase.

Further investigation of the structure of the X phase is continuing.

The research was partly funded by SCI*0291 and HCM930353 projects of the European Commission for which the Dublin group is extremely grateful. Professor B K P Scaife is thanked for useful discussions.

References

[1] Beresnev L A, Blinov L M, Osipov M A and Pikin S A 1988 *Mol. Cryst. Liq. Cryst.* A **158** 3–150

[2] Chandani A D L, Gorecka E, Ouchi Y, Takezoe H and Fukuda A 1989 *Japan. J. Appl. Phys.* **28** L1261, L1265

[3] Gorecka E, Chandani A D L, Ouchi Yu, Takezoe H and Fukuda A 1990 *Japan. J. Appl. Phys.* **29** L131

[4] Orihara H and Ishibashi Yo 1990 *Japan. J. Appl. Phys.* **29** L115

[5] Bak P and Bruinsma R 1982 *Phys. Rev. Lett.* **49** 249
[6] Yamashita M and Miyazima S 1993 *Ferroelectrics* **148** 1–9
[7] Prost J and Bruinsma R 1993 *Ferroelectrics* **148** 25–9
[8] Isozaki T, Fujikawa T, Takezoe H, Fukuda A, Hagiwara T, Suzuki Y and Kawamura I 1992 *Japan. J. Appl. Phys.* **31** L1435
[9] Isozaki T, Fujikawa T, Takezoe H, Fukuda A, Hagiwara T, Suzuki Y and Kawamura I 1993 *Phys. Rev.* B **48** 13 439
[10] Fukuda A, Takanishi Y, Isozaki T, Ishikawa K and Takezoe H 1994 *J. Mater. Chem.* **4** 997–1016
[11] Nishiyama I and Goodby J W 1992 *Proc. 14th ILCC (Pisa)* Abstracts p 269
[12] Vaksman V M and Panarin Yu P 1992 *Mol. Mater.* **1** 147
[13] Hiraoka K, Taguchi A, Ouchi Yu, Takezoe H and Fukuda A 1990 *Japan. J. Appl. Phys.* **29** L103
[14] Kocot A, Wrzalik R, Vij J K, Brehmer M and Zentel R 1994 *Phys. Rev.* B **50** 16 346–56
[15] Čopič M, Heppke G, Hollidt J M, Lozsch and Žekš B 1993 *Ferroelectrics* **147** 159–70
[16] Hiraoka K, Takanishi Y, Skarp K, Takezoe H and Fukuda A 1992 *Japan. J. Appl. Phys.* **30** L1819